Astron. Astrophys. 318, 308–314 (1997)

ASTRONOMY AND ASTROPHYSICS

Orbital evolution of high-altitude balloon satellites

Alexander V. Krivov[1] **and Juan Getino**[2]

[1] Astronomical Institute, St. Petersburg University, Stary Peterhof, 198904 St. Petersburg, Russia (krivov@aispbu.spb.su)
[2] Departamento de Matematica Aplicada Fundamental, Facultad de Ciencias, E-47005 Valladolid, Spain (getino@hp9000.uva.es)

Received 20 November 1995 / Accepted 10 June 1996

Abstract. We investigate the motion of artificial satellites with large area-to-mass ratios in high-altitude low inclined orbits, perturbed simultaneously by solar radiation pressure and Earth's oblateness. Our study is based on recent theoretical advances in circumplanetary dust dynamics (Hamilton & Krivov 1996). Applying these methods to the motion of balloon satellites, we write down and analyze the orbit-averaged equations of motion in planar approximation. Contrary to many previous works, our consideration imposes no restrictions on eccentricities and radiation pressure strengths. The results show how the eccentricity and apses line of a satellite orbit evolve with time for various area-to-mass ratios, geocentric distances, and initial data. Our special interest is with complicated dynamical effects arising from the two perturbing forces above. We demonstrate the possibility of dramatic orbital changes under small variations of initial data and force parameters. For typical balloon satellite parameters, these unusual effects may take place at altitudes between one and two Earth's radii.

Key words: space vehicles – balloons – radiation pressure – Earth's oblateness – celestial mechanics

1. Introduction

Research in dynamics of balloon-type satellites received considerable attention since late 1950s – early 1960s, stimulated by successful design and launch of such satellites as Echo-1, Echo-2, Dash 2, Pageos (e.g. Prior 1970, 1972). The gross features of dynamics of satellites with large area-to-mass ratios at high altitudes can be well understood by taking into account two dominating perturbing forces: direct solar radiation pressure and the quadrupole term in the geopotential expansion. This problem was examined in a bulk of literature, starting from pioneering works by Musen (1960), Musen et al. (1960), Parkinson et al. (1960), Kozai (1961), Brower (1963), Polyakhova (1963), and others. It is worthy of mentioning that one of the most powerful analytical methods of celestial mechanics, that of Lie transforms, has been designed by Hori (1966) while considering this problem!

Most of the previous research, however, placed at least one of the two following limitations. In some papers, radation pressure force is assumed to be weak enough. In others, the orbital eccentricity of a satellite is limited to relatively small values. Either of these restrictions drastically simplified the construction of analytic theories of motion of specific satellites and allowed the authors to advantageously use a variety of asymptotic methods in finding approximate analytic solutions to the equations of motion. Our intention is to lift both limitations above and to carry out qualitative analysis of the orbital evolution of a satellite which is affected by arbitrarily strong radiative force and may develop arbitrarily large orbital eccentricities.

This paper pretends neither to give an analytic treatment with full account of a variety of dynamical effects acting on a satellite, nor to construct an analytic theory that would describe the motion of any particular satellite among those already orbiting the Earth. Instead, we consider a relatively simple *ideal* problem that can be attacked analytically without approximations, such as the small parameter method. Our specific goal is to show, on the base of recent theoretical advances in the photogravitational problem, the possibility of previously unexpected nonlinear effects arising from the coupling of the two disturbing forces indicated above. Hence we only would like to call attention of the researchers to intricate features we have revealed in the old dynamical problem.

2. Formulation of the problem

We will consider the following ideal problem. A satellite is assumed to be spherically-symmetric. We take into account two perturbing forces: those due to oblateness of the Earth and solar radiation pressure. Other forces and processes affecting the motion of a satellite are ignored. Among others, we neglect higher harmonics of geopotential's expansion, luni-solar perturbations, atmospheric drag, perturbations due to the planets, electromagnetic forces, Earth-reflected radiation — on the caveat that these effects may be important, if not essential, for accurate prediction of the orbits of specific balloons (see, e.g., Prior 1970, 1972;

Send offprint requests to: A.V. Krivov

Slowey 1969, 1974 a, b; Römer & Wulf-Mathies 1974 and references therein). We will consider the planar problem only. It means that we set Earth's obliquity 23.5° to zero and suppose the orbital plane of a satellite to be equatorial. Next, we adopt circular Earth's orbit around the Sun. Finally, we will deal with an orbit-averaged problem and therefore neglect short-periodic terms in orbital elements of a satellite.

In Sect. 5, we will revert to some of these simplifications and assumptions and check that actual motion of a satellite can be closely approximated by our simplified model.

3. Equations of motion

The planar problem is described by four orbital elements: semimajor axis a, eccentricity e, longitude of pericenter $\tilde{\omega}$, and mean anomaly M. The semimajor axis a is not subject to secular changes, until the shadowing effects are included (e.g. Allan 1962), and can be treated as a given parameter. "Fast" variable M defines the position of a satellite in its orbit and does not characterize the orbit itself. Hence we should follow the evolution of two elements: eccentricity and longitude of pericenter. Instead of the latter, it is more convenient to use solar angle, $\phi_\odot \equiv \tilde{\omega} - \lambda_\odot$ ($\lambda_\odot$ stands for the true longitude of Sun). This variable has a clear physical meaning of angular distance between the pericenter and direction toward the Sun. As independent variable, we will use $\lambda_\odot$ which, since the Earth's orbital eccentricity is neglected, is a linear function of time.

The orbit-averaged equations for e and $\phi_\odot$ were derived in studies of circumplanetary dust dynamics (Hamilton 1993; Krivov et al. 1996; Hamilton & Krivov 1996) and have the form

$$\begin{aligned} \frac{de}{d\lambda_\odot} &= C\sqrt{1-e^2}\sin\phi_\odot \\ \frac{d\phi_\odot}{d\lambda_\odot} &= C\frac{\sqrt{1-e^2}}{e}\cos\phi_\odot + \frac{W}{(1-e^2)^2} - 1. \end{aligned} \tag{1}$$

These equations are governed by two dimensionless parameters that characterize the strength of the perturbing forces: radiative parameter C and oblateness parameter W. The first of them is defined as

$$C = \frac{3}{2}\sigma\frac{n}{n_\odot},$$

where n and $n_\odot$ are mean motions of satellite and Sun, and σ is the ratio of radiative force to Earth's gravity

$$\sigma = \frac{F_{pr}}{F_{gr}} = \frac{F_\odot a^2}{GMc}\gamma.$$

Here, $F_\odot$ is the solar flux at 1 AU, GM is the gravitational parameter of the Earth, c is the speed of light, and γ is the area-to-mass ratio of the satellite. We assume the reflectance factor to be unity that corresponds to either complete reflectance or full absorption.

The oblateness parameter W is introduced as

$$W \equiv \frac{3}{2}J_2\left(\frac{R}{a}\right)^2\frac{n}{n_\odot},$$

where J_2 and R denote the 2nd zonal harmonic coefficient and equatorial radius of the Earth, respectively. This parameter is obviously the function of a only; numerically, $W = 1$ at $a = 1.94R$. Its physical meaning is also transparent: the product $n_\odot W$ equals the precession rate of $\tilde{\omega}$ due to J_2 for nearly circular orbit.

System (1) can be written in a quasi-canonical form (Kholshevnikov 1995; Krivov et al. 1996; Hamilton & Krivov 1996)

$$\frac{de}{d\lambda_\odot} = -\frac{\sqrt{1-e^2}}{e}\frac{\partial\mathscr{H}}{\partial\phi_\odot}, \qquad \frac{d\phi_\odot}{d\lambda_\odot} = \frac{\sqrt{1-e^2}}{e}\frac{\partial\mathscr{H}}{\partial e} \tag{2}$$

with the autonomous "Hamiltonian"

$$\mathscr{H} = \sqrt{1-e^2} + Ce\cos\phi_\odot + \frac{W}{3}(1-e^2)^{-3/2} \tag{3}$$

and admits an integral of the motion

$$\mathscr{H}(e,\phi_\odot) = const \tag{4}$$

that makes the system (2)–(3) integrable in quadratures.

4. Stationary points of the Hamiltonian

The structure of the phase space $(e,\phi_\odot)$ and the properties of solutions of Eqs. (2)–(3) are essentially determined by stationary points of the Hamiltonian $\mathscr{H}$, $\partial\mathscr{H}/\partial e = \partial\mathscr{H}/\partial\phi_\odot = 0$. The complete qualitative analysis has been performed in (Hamilton & Krivov 1996) and resulted in the following.

1. There always exist two stationary points of $\mathscr{H}$ (fixed saddles): $P_1 = (0, 90°)$ and $P_2 = (0, 270°)$.

2. At most two additional equilibrium points may exist at $\phi_\odot = 0$. Introducing the function

$$\mathscr{H}_0(e) \equiv e(1-e^2)^{-1/2}\left[W(1-e^2)^{-2} - 1\right] \tag{5}$$

with the minimum at

$$e_- = \sqrt{1 + 2W - \sqrt{4W^2 + 5W}} \qquad (0 < W < 1),$$

the existence conditions for these points can be written as follows. If $C < -\mathscr{H}_0(e_-)$, then there exist two points: $P_3 = (e_3, 0)$ (maximum) and $P_4 = (e_4, 0)$ (saddle). If $C = -\mathscr{H}_0(e_-)$, then there exists one point $P_3 = (e_3, 0)$ (saddle). If, finally, $C > -\mathscr{H}_0(e_-)$, then the additional points at $\phi_\odot = 0$ are absent.

3. The fifth stationary point $P_5 = (e_5, 180°)$ (local minimum of the Hamiltonian) always exists regardless of the parameter values.

5. Phase portraits and types of satellite motion

Depending on the number of equilibrium points, different topological types of phase portraits are possible. A particular attention will also be paid to a phase trajectory associated with an initially circular orbit — *the* $e = 0$ *trajectory*. Accordingly, we suggest a classification of phase portraits presented in Table 1.

Table 1. Classification of phase portraits

Phase portrait type	Equilibrium points of $\mathscr{H}$	The $e = 0$ trajectory	Figures
I	P_1, P_2, P_3, P_4, P_5	embraces P_3	2a,b,c
II	P_1, P_2, P_3, P_4, P_5	passes through P_4	2d
III	P_1, P_2, P_3, P_4, P_5	embraces P_5	2e,f,g
IV	P_1, P_2, $P_3 = P_4$, P_5	embraces P_5	2h
V	P_1, P_2, P_5	embraces P_5	2i,j

Five types of portraits are distinguished by a set of stationary points and by a behavior of the $e = 0$ trajectory.

Now we come to the description of different phase portrait types. We fix initial semimajor axis of satellite's orbit and will gradually increase area-to-mass ratio γ of a hypothesized satellite; this corresponds to growth of radiative parameter C under the constant oblateness parameter W. As γ (or C) grows up, the number and locations of stationary points change, and we observe sequentially all the types from I to V. To be more specific, we set $a = 2.5R$ throughout the description that follows. The dynamical histories of eccentricity for satellites with different area-to-mass ratios being launched into initially circular orbits are plotted in Fig. 1; the phase portraits for the same values of γ are given in Fig. 2. The data for these figures were calculated by numerical integrations of Eq. (1) which had been previously transformed to nonsingular variables $e\sin\phi_\odot$, $e\cos\phi_\odot$.

1. While C is small (the radiative force is weak enough), the phase portrait is of the type I (Fig. 2 a,b,c). All five equilibrium points P_1 to P_5 are present. The $e = 0$ trajectory shows periodic oscillations of eccentricity, with amplitude increasing and period diminishing as C is growing up (Fig. 1 a,b,c). The solar angle for the $e = 0$ trajectory librates between $-90°$ and $90°$. For trajectories with initial $e \neq 0$, the eccentricity changes periodically, and the solar angle may either librate or rotate, depending on the initial e and $\phi_\odot$. Stable orbits with $e = const$ and $\phi_\odot = const$ exist at the points P_3 and P_5.

2. At a certain value of C, we observe the "degenerate" type II (Figs. 1d and 2d). It separates the types I and III and represents a fast change in the phase geometry — *transition of the* $e = 0$ *trajectory*. It should be stressed that three types I, II, and III have qualitatively the same set of five stationary points and they are distinguished by the behavior of the $e = 0$ trajectory only. For the type I ("before" the transition), the $e = 0$ trajectory surrounds the maximum P_3, whereas the separatrix passing through the saddle P_4 embraces the minimum P_5 (Fig. 2c). At the transition point (type II), the $e = 0$ trajectory coincides with the saddle separatrix (Fig. 2d). "After" the transition (type III), the $e = 0$ trajectory surrounds the minimum P_5, and the separatrix starting from P_4 embraces the maximum P_3 (see Fig. 2e).

Perhaps the most interesting feature of the transition in question is a jump in both amplitude and period of eccentricity variations for an initially circular orbit. In our numerical example, the maximum eccentricity jumps from 0.5 to 0.8 under a tiny change in C! It is illustrated by Figs. 1 b,c,d that give eccentricity versus time, and by Figs. 2 b,c,d that provide eccentricity–solar angle dependencies "before" and "after" the transition. This phenomenon was independently pointed out by several authors (Hamilton 1996; Ishimoto 1996; Krivov et al. 1996) when studying a quite different problem of motion of dust grains ejected from the martian moon Phobos.

3. Still larger values of γ (or C) lead to phase portraits of the type III (Fig. 2 e,f,g). For the $e = 0$ trajectory, e changes periodically (but not sinusoidally as for the type I), and $\phi_\odot$ librates between 90° and 270° (Fig. 1 e,f,g).

4. Next degenerate case, type IV, which lies between the types III and V, represents the merging of two stationary points P_3 and P_4 and takes place when $C = -\mathscr{H}_0(e_-)$. This effect, to be called *bifurcation of stationary points*, is clear from a comparison of Figs. 2g (type III), 2h (type IV), and 2i (type V). Interestingly, the change in number of stationary points in the phase space is not attended by an appreciable change in the behavior of the $e = 0$ trajectory. For this reason, the bifurcation of stationary points causes less pronounced effect in numerical integrations of satellite's motion than the transition of $e = 0$ trajectory.

5. After the bifurcation, the portraits are of the type V (Fig. 2 i,j). The points P_3 and P_4 have disappeared. The eccentricity varies periodically and its maximum value is not less than e_5 regardless of the initial data; consequenlty the orbits develop substantial eccentricities (Fig. 1 i,j). Both librational and rotational regimes of the solar angle evolution are possible, depending on the initial e and $\phi_\odot$.

We wish now to determine which types of the motion correspond to specific values of semimajor axis and area-to-mass ratio. According to (Hamilton & Krivov 1996), the transition of $e = 0$ trajectory occurs when C and $e \equiv e_4$ satisfy the equations

$$\mathscr{H}(e_4, 0) = \mathscr{H}(0, \pi/2), \qquad \mathscr{H}_0(e_4) = -C, \tag{6}$$

and the bifurcation of stationary points takes place for C and $e \equiv e_3$ such that

$$d\mathscr{H}_0(e_3, 0)/de = 0, \qquad \mathscr{H}_0(e_3) = -C. \tag{7}$$

In Table 2, we present the results of the numerical solution of Eqs. (6) and (7) for various semimajor axes of satellite's orbits. In Fig. 3, we show in the (a, γ)-plane the types of motion associated with various pairs "semimajor axis — area-to-mass". Two curves in the plot correspond to the degenerate types II and IV.

From Table 2 and Fig. 3, we observe that no transitions of $e = 0$ trajectory or bifurcations are possible when satellite orbits the Earth closer than at 1.94 its radii; the motion is then of the type V. For more distant satellites, all the types may take

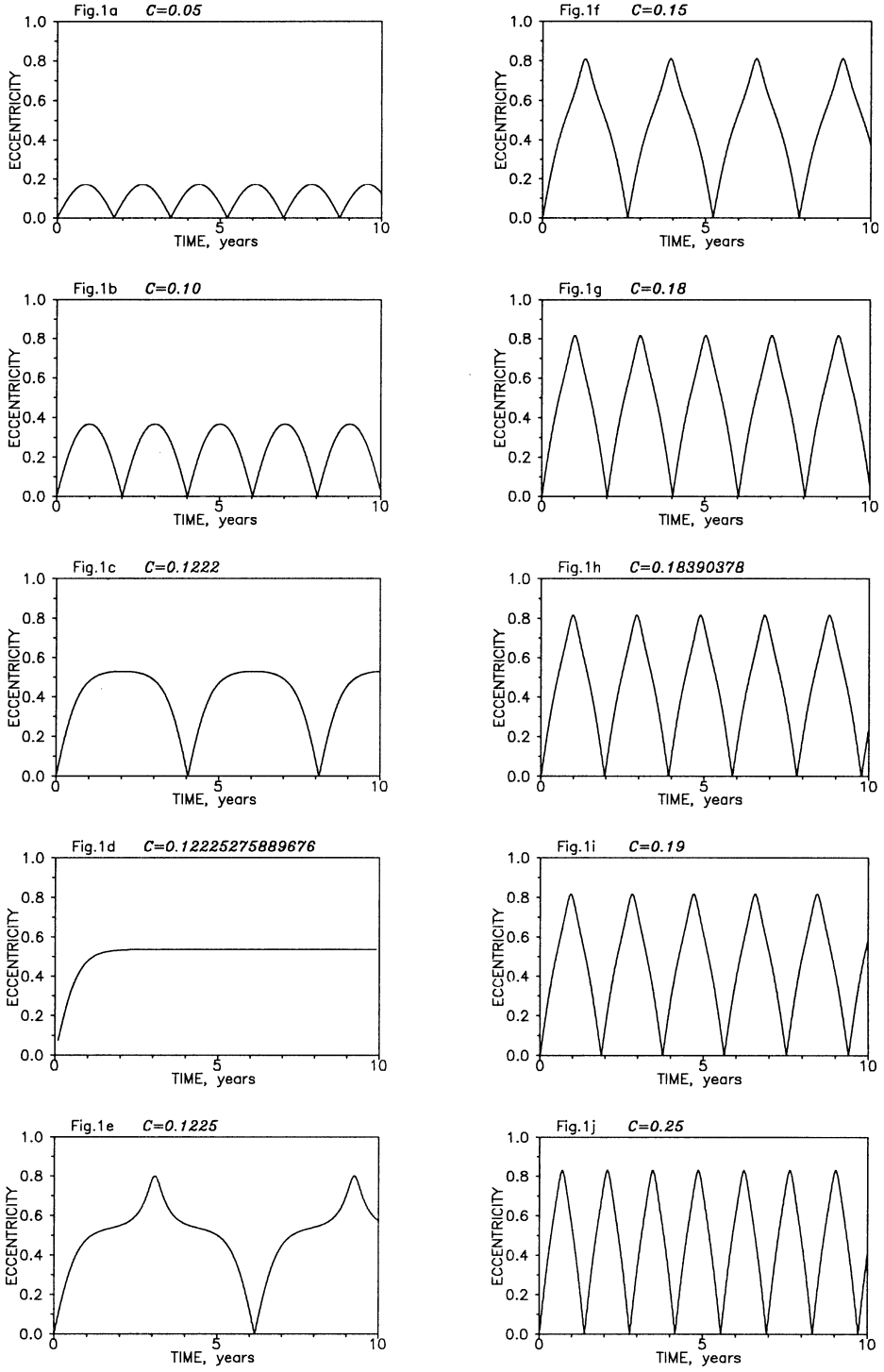

Fig. 1a–j. Evolution of eccentricity for satellites with different area-to-mass ratios initially in circular orbits. Semimajor axis is 2.5 Earth's radii that corresponds to the oblateness parameter $W = 0.409$.

place. However, for satellites with semimajor axis larger than crudely 3 Earth's radii, the changes in phase topology occur at unrealistically large area-to-mass ratios. At these distances, the phase portraits for satellites with typical γ would be of the type I.

Recall that we performed our analysis for an ideal problem implying a set of simplifications and assumptions (Sect. 2). Of these simplifications, the most serious are: (i) we have neglected Earth's obliquity 23.5°, and (ii) we have ignored the shadowing effects. This gives rise to the following question: does our model, including subtle effects such as bifurcations, work, though for equatorial orbits? To get the answer, we undertook a set of special checks. We numerically integrated 3D (spatial) equations of motion in cartesian coordinates which were then converted into osculating elements. In these integrations, the actual Earth obliquity of 23.5° was included. Besides, we accounted for planetary shadow and used a more realistic force model with solar gravity perturbations. Since we integrated the equations in co-

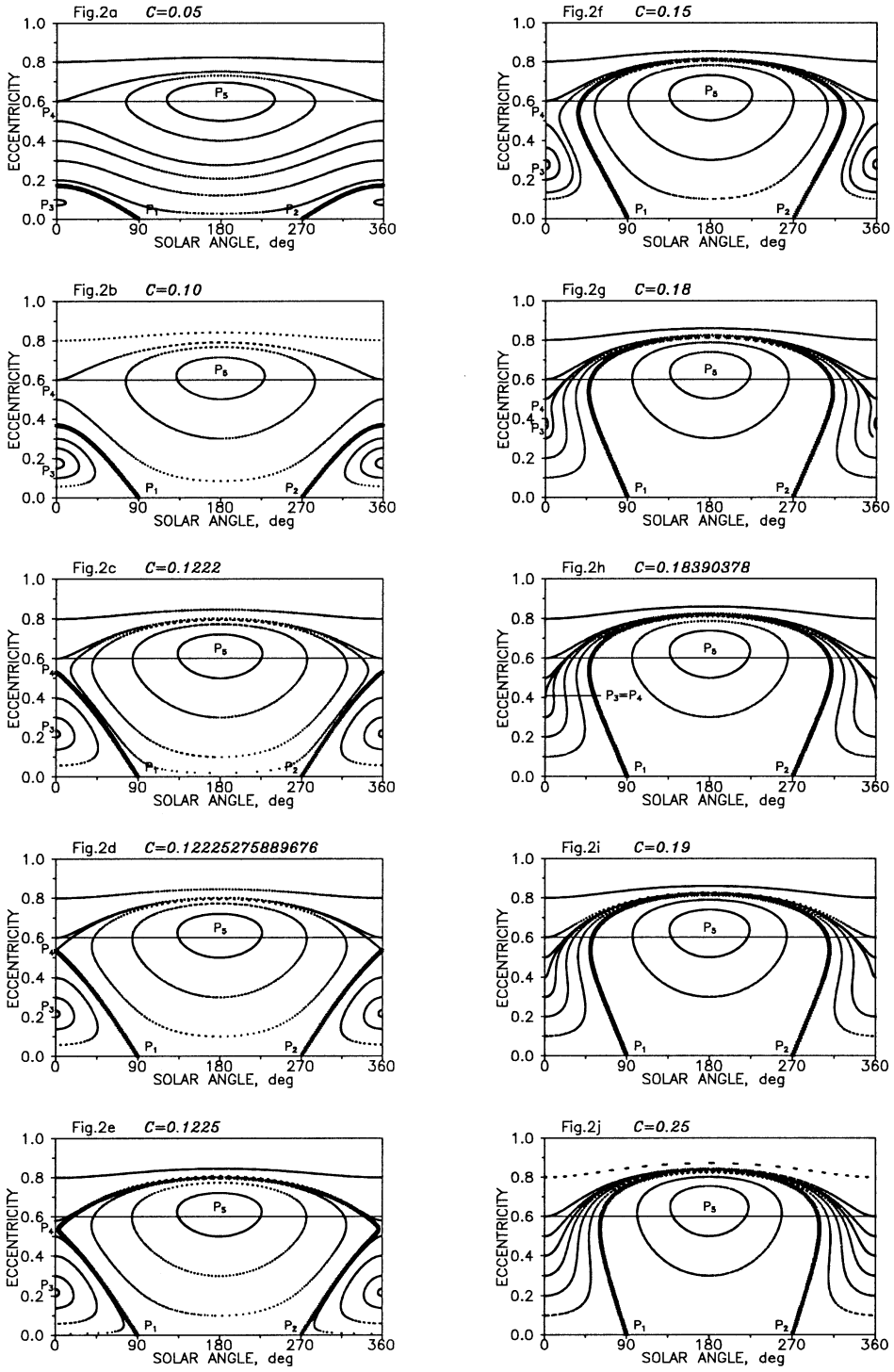

Fig. 2a–j. Phase portraits (eccentricity versus solar angle) for the same satellites as in Fig. 1. The horizontal line marks the critical eccentricity $e = 0.6$, for which the perigee lies at the Earth surface. The thick line depicts the $e = 0$ trajectory. A sequence of plots presents different types of phase portraits.

ordinates rather than orbit-averaged equations in elements, this was also a test for validity of orbit-averaging procedure.

The results definitely show that the main features of the dynamics do survive. The phase space holds the same structure as described above. The transitions of $e = 0$ trajectory and bifurcations take place as well, although at slightly shifted values of the parameters.

Of all the integration results, we reproduce three plots for $e(t)$ (Fig. 4). The values of parameter C chosen are close to those associated with the transition of $e = 0$ trajectory. Solid/dashed lines depict the results obtained with/without consideration of shadowing. The panels a, b, and c may be compared with Fig. 1c, e, and f. It is seen that the planar model really provides a good approximation to a realistic spatial problem.

Since the spatial problem is no longer integrable, quite complicated effects such as switches between topological types near the intersection of separatrices may occur. For some values of C and W, and for certain initial data, numerical integrations

Table 2. Critical values of parameters. The area-to-mass ratio γ is measured in $\mathrm{cm}^2\ \mathrm{gr}^{-1}$

a/R	W	Transition of $e = 0$ trajectory			Bifurcation of stationary points		
		γ	C	e_4	γ	C	$e_3 = e_4$
1.95	0.976	1.2	0.001	0.090	1.7	0.001	0.064
1.96	0.959	2.7	0.002	0.119	3.9	0.002	0.084
1.97	0.942	4.6	0.003	0.142	6.5	0.004	0.101
1.98	0.925	6.7	0.004	0.161	9.5	0.006	0.115
1.99	0.909	9.0	0.006	0.179	12.8	0.008	0.127
2.00	0.893	11.5	0.007	0.194	16.4	0.010	0.139
2.05	0.819	25.9	0.016	0.258	37.1	0.023	0.186
2.10	0.753	42.2	0.026	0.307	60.7	0.038	0.223
2.20	0.640	77.2	0.050	0.385	112.3	0.072	0.284
2.30	0.548	112.6	0.074	0.445	165.6	0.109	0.333
2.40	0.472	146.7	0.098	0.495	218.2	0.146	0.376
2.50	0.409	178.9	0.122	0.537	269.1	0.184	0.413
2.60	0.357	208.8	0.146	0.574	317.7	0.222	0.447
2.70	0.312	236.4	0.168	0.606	364.0	0.259	0.477
2.80	0.275	261.9	0.189	0.634	408.0	0.295	0.505
2.90	0.243	285.2	0.210	0.659	449.6	0.331	0.530
3.00	0.216	306.6	0.230	0.682	489.0	0.366	0.554

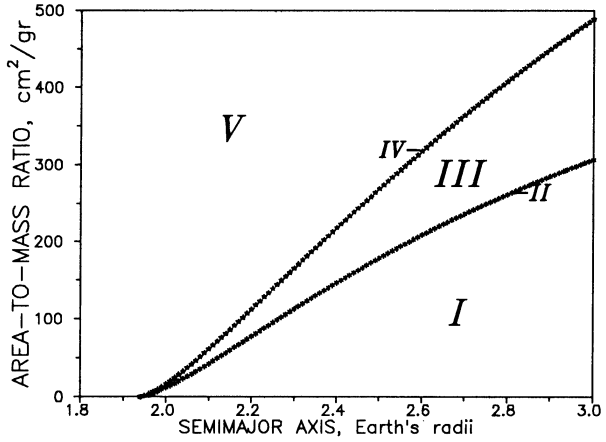

Fig. 3. Relation between a pair "semimajor axis — area-to-mass ratio" and type of a phase portrait. Two curves in the plot correspond to degenerate types II and IV.

exhibit a chaotic orbital behavior. The eccentricity oscillations of the type I (like in Fig. 1c) alternate with those of the type III (similar to Fig. 1e). Moreover, a small change in the initial data/parameters/force model would alter the order in which two types of oscillations appear in the succession of periods! A comprehensive investigation of these intricate stochastic features may be the subject of a separate study.

6. Conclusions and discussion

We considered the motion of a light spherical Earth's satellite perturbed together by direct pressure of solar radiation and 2nd zonal harmonic of the geopotential. We used the orbit-averaged equations of motion and the results of their qualitative analysis presented in (Hamilton & Krivov 1996) to examine the evolution of eccentricity and perigee orientation. Throughout the study, we did not place any restrictions on the orbital eccentricity and the area-to-mass ratio of a satellite, both of which may be arbitrarily large.

Our results show how the eccentricity and apses line of a satellite orbit evolve with time for various area-to-mass ratios, geocentric distances, and initial data. We can recognize three zones with respect to the geocentric distance of a satellite.

Satellite orbits with $a < 1.94R$ (with altitudes $\lesssim 6000$ km) but not appreciably subjected to atmospheric drag form the near zone where the motion is of the type V according to our classification. All balloon-type satellites launched so far orbited the Earth in this zone; note, e.g., Echo 1 with $a \sim 8000$ km or Pageos with $a \sim 10600$ km.

Satellites that orbit the Earth at $a \gtrsim 3R$ (with altitudes $\gtrsim 13000$ km) would lie in the far zone and, for area-to-mass ratios of order $100\ \mathrm{cm}^2\ \mathrm{gr}^{-1}$, the phase portraits would be of the type I. We should note, however, that for the most distant orbits the model presented here is no longer adequate, due to significant luni-solar perturbations. Therefore, one should consider the "radiation pressure + luni-solar force" problem instead of "radiation pressure + oblateness" one that we examined. Such a study can be accomplished in analogous way, because the problem in question also admits a quasi-Hamiltonian formulation and can be integrated in closed form (see Hamilton & Krivov 1996 for details).

Finally, the intermediate zone ($2R \lesssim a \lesssim 3R$) is the place where our model best applies to the description of satellite's motion. Balloon satellites, if launched into these orbits, would exhibit the most interesting dynamics. All five types of motion are possible here, and small variations of initial data and force parameters would cause transitions between the types that may result in sharp orbital changes. That is to say, this zone represents "the dangerous place" for balloon satellites because, for some

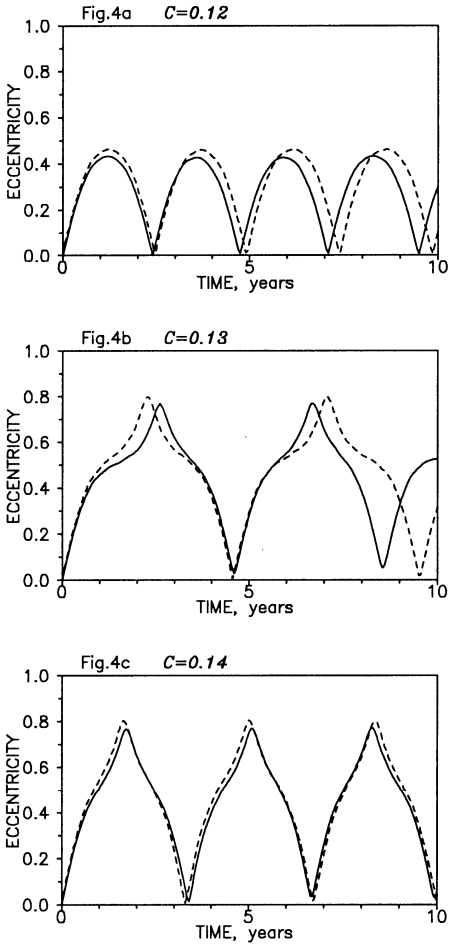

Fig. 4a–c. Evolution of eccentricity near the transition of the $e = 0$ trajectory. The panels **a**, **b**, and **c** are similar to Fig. 1c,e, and f, but derived from numerical integrations of spatial equations of motion, i.e. with actual Earth's obliquity 23.5°. The satellite orbits are initially circular and equatorial; the semimajor axis is 2.5 Earth's radii. Solid lines: shadowing is taken into account; dashed lines: shadowing is ignored.

values of parameters and initial data, very unstable orbits are possible.

Acknowledgements. We thank K.V. Kholshevnikov and L.L. Sokolov for constructive remarks. A.K. was supported by the Young Scientists Program grant 137-3-2.2 of St. Petersburg Government. J.G. has been partially supported by CICYT, Project No. ESP93–741.

References

Allan R.R., 1962, Quart. J. Mech. and Appl. Math. 15, 283
Brower D., 1963. In: Roy M. (ed.) Dynamics of Satellites. Academic Press, New York, p. 34
Hamilton D.P., 1993, Icarus 101, 244. Erratum: Icarus 103, 161
Hamilton D.P., 1996, Icarus 119, 153
Hamilton D.P., Krivov A.V., 1996, Icarus (in press)
Hori G., 1966, Space Math. Part 3, Providence, RI, Amer. Math. Soc., 167
Ishimoto H., 1996, Icarus (in press)
Kozai Y., 1961, Smithsonian Astrophys. Obs. Spec. Rept., No. 56, 1
Kholshevnikov K.V., 1995, private communication
Krivov A.V., Sokolov L.L., Dikarev V.V., 1996, Cel. Mech. Dyn. Astron. (in press)
Musen P., 1960, J. Geophys. Res. 65, 1391
Musen P., Bryant R., Bailie A., 1960, Sci 131, 935
Parkinson R.W., Jones H.M., Shapiro I.I., 1960, Sci 131, 920
Polyakhova E.N., 1963, Bull. Inst. Theor. Astron. Acad. Sci. USSR, 9, 15 (in Russian)
Prior E.J., 1970. In Morando B. (ed.) Dynamics of Satellites. Springer, Berlin, p. 303
Prior E.J., 1972. In Use Artif. Satellites Geod. Washington, D.C., p. 196
Römer M., Wulf-Mathies C., 1974. Zeitschrift für Geophysik, 40, 625.
Slowey J.W., 1969. In Space Res., 9 Proc. Springer, Berlin, p. 76
Slowey J.W., 1974 a. In Space Res., 14 Proc. Springer, Berlin, p. 143
Slowey J.W., 1974 b. Smith. Astr. Obs. Sp. Rep. No. 356, 1

This article was processed by the author using Springer-Verlag LaTeX A&A style file *L-AA* version 3.